Analytica Chimica Acta 1159 (2021) 338382

Contents lists available at ScienceDirect

Analytica Chimica Acta

journal homepage: www.elsevier.com/locate/aca

Anti-pesticide DNA aptamers fail to recognize their targets with asserted micromolar dissociation constants

Lorena Zara [a, b], Silvia Achilli [a], Benoît Chovelon [a, c], Emmanuelle Fiore [a], Jean-Jacques Toulmé [b], Eric Peyrin [a, **], Corinne Ravelet [a, *]

[a] Univ. Grenoble Alpes, CNRS, DPM, 38000, Grenoble, France
[b] Novaptech, 2 Allée Du Doyen Georges Brus, 33600, Pessac, France
[c] Service de Biochimie, Biologie Moléculaire, Toxicologie Environnementale, CHU de Grenoble-Alpes Site Nord- Institut de Biologie et de Pathologie, La Tronche, France

HIGHLIGHTS

- The molecular recognition capability of two anti-pesticide aptamers were investigated through fluorescent and ITC approaches.
- They did not specifically bind in solution with the reported micromolar dissociation constants.
- This work highlighted the need to validate the aptamer-target interaction by using multiple characterization strategies.

GRAPHICAL ABSTRACT

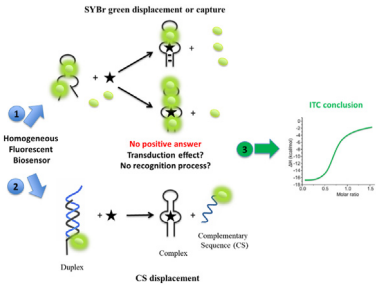

ARTICLE INFO

Article history:
Received 20 January 2021
Received in revised form
7 March 2021
Accepted 8 March 2021
Available online 20 March 2021

Keywords:
Pesticide
Aptamers
Fluorescence anisotropy
Isothermal titration calorimetry

ABSTRACT

Herein, we originally aimed at developing fluorescence anisotropy biosensor platforms devoted to the homogeneous-phase detection of isocarbophos and phorate pesticides by using previously isolated DNA aptamers. To achieve this, two reporting approaches displaying very high generalizability features were implemented, based on either the complementary strand or the SYBR green intercalator displacement strategies. Unfortunately, none of the transduction methods led to phorate-dependent signals. Only the SYBR green displacement method provided a small output in the presence of isocarbophos, but at an analyte concentration greater than 100 μM. In order to identify the origin of such data, isothermal titration calorimetry (ITC) experiments were subsequently performed. It was shown that aptamers bind neither isocarbophos nor phorate in free solution with the claimed micromolar dissociation constants. This work puts forward some doubts about the previously described aptasensors that rely on the use of these functional DNA molecules. It also highlights the need to carefully investigate the binding capabilities of aptamers after their isolation and to include appropriate control experiments with scrambled or mutated oligonucleotides.

* Corresponding author.
** Corresponding author
E-mail addresses: eric.peyrin@univ-grenoble-alpes.fr (E. Peyrin), corinne.ravelet@univ-grenoble-alpes.fr (C. Ravelet).

https://doi.org/10.1016/j.aca.2021.338382
0003-2670/

1. Introduction

The usage of pesticides in agriculture is well-known to cause very serious problems in the food and environment contamination, putting the health of humanity at risk [1]. Indeed, organophosphorous pesticides (OP), the most used pesticides, vary in their toxicities [2], but most of them are poisonous and can cause acute or chronic damage to humans.

Currently, the methods used for pesticide detection generally imply gas chromatography, liquid chromatography, and liquid or gas chromatography coupled to mass spectrometry detection (HPLC-MS, GC-MS) [3–5]. Although these approaches are sensitive and trustworthy, most of them are complicated, time consuming, and expensive, and require highly qualified technicians [6]. Thus, rapid, sensitive, specific, and easy-to-use analytical methods are being developed to meet the need for environmental pollution control and early warning. Biosensors are promising in this context due to their advantages of low cost, easy operation, fast response, and high sensitivity. As compared with common antibodies or enzymes used in elaborating biosensors, aptamers display better stability, lower molecular weight, easy modification and low cost, and are considered as excellent candidates for developing aptasensors devoted to the pesticide detection. Hence, there is a great interest for designing new aptasensors able to detect pesticide residues [7] and, to that end, a large number of pesticide-binding aptamers have been recently selected [8].

Among them, DNA aptamers that bind to four OP isocarbophos, phorate, omethoate and profenofos have been reported in 2012 by Wang and colleagues [9]. *In vitro* selection was performed on the basis of the structure-switching method using an immobilized random ssDNA library. Two ssDNA sequences, **SS2-55 and SS4-54**, were identified. The authors stated that the apparent dissociation constant between the functional DNA molecules and the four organophosphorus pesticides lies between 0.8 and 2.5 μM. The same authors have subsequently engineered a series of variants that better interact with OP [10]. A molecular beacon (MB) was used for the competitive binding to aptamers and the fluorescence intensity changes of MB was calculated as inhibition ratio. Among them, the aptamer **SS-24–35** obtained from a construct of **SS2-55** and **SS4-54** displayed the highest activity in binding to isocarbophos and profenofos with inhibition ratios of over 85% and 70%, respectively.

These three aptamers, adsorbed or grafted on a sensing surface, have been employed in the design of various heterogeneous-phase biosensors. In 2014, Pang et *al*. developed a rapid Surface Enhanced Raman Spectroscopy (SERS) method to detect and discriminate four specific pesticides (isocarbophos, omethoate, phorate, and profenofos) by using the immobilized **SS2-55** aptamer [11]. More recently, the surface-grafted **SS24–35** aptamer was applied for developing an electrochemical aptasensor to sense the profenofos, phorate, isocarbophos and omethoate analytes [12]. Most attention was focused on the design of colorimetric nanoparticle-based aptasensors. For instance, the detection of six OP (isocarbophos, phosalone, methamidophos, acephate, trichlorfon, dursban) [13], or phorate [14], was achieved with the **SS2-55** aptamer adsorbed or grafted onto gold nanoparticles (AuNP) surfaces. **SS2-54** and **SS24–35** aptamers were respectively used for AuNP colorimetric detection of isocarbophos [15] and omethoate [15,16]. Li et al. also described an aptasensor for the determination of phorate based on **SS2-55**-templated silver nanoclusters [17].

Among aptamer-based sensors, homogeneous-phase platforms such as fluorescent sensors are very performing, due notably to their high intrinsic sensitivity, high efficiency, simplicity, speed and the capability for automated high-throughput and multiplexed analysis [18–20]. To date, only one study by Zhang et al. [10] has focused on the design of FRET-based DNA aptasensors for the isocarbophos and phorate determination. Thereby, the original aim of this study was to elaborate fluorescence anisotropy (FA) systems that would be capable to sense these two OPs. The measurement by FA adds another dimension of observation to the fluorescence-based experiment, providing information on the local environment, fluorescence lifetime and molecular mass. One of the advantages of fluorescence anisotropy studies as compared to fluorescence intensity (FI) ones is that since the measurements are ratiometric in nature, they are not dependent on the actual light intensity values or the fluorophore concentration.

To achieve our goal, we decided to implement two reporting strategies that exhibit the most desirable features in terms of assay generalizability, *i. e.* based on displacement schemes that involve either a complementary stand of the functional oligonucleotide or a DNA intercalator (SYBR Green). These indirect approaches are characterized by their easiness and broad applicability, regardless of aptamer structure. Indeed, significant FA responses have been reported for hairpin (ATP and Hg(II) detection) [21], quadruplex (ochratoxin A detection) [22], or unknown (tyrosinamide detection) [23] motifs.

Unfortunately, regardless the used approach, we found that the afore described OP aptamers did not respond to the presence of analytes with the apparent affinities claimed by the authors. Well-validated small-molecule aptamers directed against L-tyrosinamide, D-arginine-vasopressin or ochratoxin A were concomitantly tested to confirm the generalizability of the FA-displacement methods used. ITC experiments were then carried out to ascertain whether the tested aptamers recognize OP compounds with the reported micromolar dissociation constants. We found that the DNA oligonucleotides (in the micromolar concentration range) are unable to interact with the analytes, even at a concentration as high as 500 μM. We finally discussed the requirements to prove the proper functionality of an aptamer, with the need to multiply characterization strategies within more than one assay platform.

2. Materials and methods

2.1. Chemicals

Sodium chloride (NaCl), SYBr green I (SG), L-tyrosinamide (L-Tym), ochratoxin A (OTA) were purchased from Sigma-Aldrich (Saint-Quentin, France). D-arginine-vasopressin (AVP) trifluoroacetate salt were supplied by Bachem (Weil am Rhein, Germany). Magnesium chloride hexahydrate ($MgCl_2$, $6H_2O$) was purchased from Fisher Scientific (Illkirch, France). HCl and NaOH were provided by Carlo Erba (Val de Reuil, France). All chemicals were at least of analytical grade. Water was purified using a Millipore (Bedford, MA) filter with a reverse osmosis cartridge.

Pesticides (isocarbophos and phorate) were purchased from Dr. Ehrenstorfer GmbH and stocked in ethanol at 4 °C at 10 mM concentration. L-Tym was prepared in water at 10 mM concentration. A stock solution of AVP was prepared at 1845 μM in water. Ochratoxin A was dissolved in methanol to obtain stock solution (2.5 mM).

All DNA samples were from Eurogentec (Seraing, Belgium), stock solutions were made at 1 mM concentration with pure water and stored at −20 °C. The sequences are listed in Table 1.

Buffers were prepared every week and stored at 4 °C. For all experiments, the oligonucleotides dedicated to pesticides or other targets were diluted in 2X or more concentrated buffer (it depends on experiments), denatured at 80 °C during 5 min, kept at room temperature for 30 min. Pesticides were added to obtain a final concentration of 5% ethanol. For all the experiments and wells, the binding buffer for **SS2-55** and **SS-24–35** aptamers dedicated to pesticides with a respective length of 55 and 35 mer, consisted of

Table 1
Oligonucleotides sequences. Complementary sequences are in green and red.

DNA names	Sequences (from 5' to 3')
SS2-55	AAGCTTGCTTTATAGCCTGCAGCGATTCTTGATCGGAAAAGGC TGAGAGCTACGC
SS-24-35	AGCTTGCTGCAGCGATTCTTGATCGCCACAGAGCT
Apt-Tym-38	TGGAGCTTGGATTGATGTGGTGTGTGAGTGCGGTGCCC
Apt-Tym-49	AATTCGCTAGCTGGAGCTTGGATTGATGTGGTGTGTGAGTGCG GTGCCC
Apt-OTA	GATCGGGTGTGGGTGGCGTAAAGGGAGCATCGGACA
Apt-AVP	TCACGTGCATGATAGACGGCGAAGCCGTCGAGTTGCTGTGTG CCGATGCACGTGA
TR-CSA	TR-CAAGAATCG
TR-CSB	CTGCAGCAA-TR
CS-Tym	TR-CACATCAAT

10 mM Tris, pH 8, 10 mM NaCl, 10 mM KCl, 10 mM $MgCl_2$ and 5% ethanol. For L-Tym assays, the buffer used was mainly composed with 10 mM Tris, pH 7.5, 25 mM NaCl, 5 mM $MgCl_2$ with 5% ethanol. For AVP, the binding buffer used was composed of 10 mM Tris, pH 7.5, 50 mM KCl, 3 mM $MgCl_2$ and 2.5% ethanol. For OTA, the binding buffer consisted of 10 mM Tris, pH 8.5, 120 mM NaCl, 5 mM KCl, 20 mM $CaCl_2$ and 2.5% ethanol.

2.2. SYBR green displacement

Titration curves of aptamers ranging from 8 to 512 nM (for **SS2-55** and **SS-24**–**35**), 1–32 nM (for Apt-Tym-38 and Apt-Tym-49), 4–8000 nM (for Apt-OTA or Apt-AVP) in the absence and in the presence of respectively 100 μM of isocarbophos and 500 μM of phorate, 100 μM of tyrosinamide, 3 μM of OTA and 500 μM of AVP were performed. After, titration curves of the targets, ranging from (0–500 μM for isocarbophos), (0–100 μM for L-Tym), (400–25 600 μM for OTA) and (6.25–100 μM for AVP) were realised with an appropriate concentration of aptamer showing the higher difference of anisotropy between aptamer alone and aptamer with target. The reagents were mixed in the wells in the following order: after denaturation, DNA aptamer and targets were first pre-incubated for 15 min at room temperature or 4 °C followed by the addition of SG. The final concentration of SG in the wells was fixed to 1.05 μM as previously reported [24]. Experiments were performed in triplicate. Reading measurement were realised immediately or after 30 min of incubation time, depending on experiments realised.

2.3. Complementary strand displacement

To establish the titration curves of aptamer (ranging from 20 nM to 1280 nM) in the presence and in the absence of isocarbophos (100 μM or 500 μM), phorate (100 μM) or L-Tym (100 μM), structured aptamers and analyte solutions were mixed into individual wells (final volume = 100 μL). After 15 min at room temperature, the complementary strand (CS) (20 nM) was added and the solution was kept at room temperature for 15 min in the dark. Blank wells of the microplate received 100 μL of the binding buffer. All experiments were done in triplicate. Finally, the microplate was placed into the microplate reader for the measurement.

2.4. Fluorescence anisotropy measurements

The fluorescence anisotropy (FA) was measured in black 96–well Greiner Bio-One microplates (Courtaboeuf, France) using a Tecan Infinite F500 microplate reader (Männedorf, Switzerland). Excitation for SG based assay was set at 485 ± 20 nm and emission was collected with 535 ± 25 nm bandpass filters. For complementary strand displacement, the measurement was done with excitation filters at 590 ± 20 nm and emission filters at 635 ± 25 nm.

Fluorescence anisotropy change Δr was calculated as follows:

$\Delta r = r - r_f$ where r is the anisotropy of the hybrid (dye-labelled CS or SG with aptamer) in presence of target and r_f is the anisotropy of the dye-labelled CS or SG with aptamer in absence of target.

2.5. ITC measurements

Calorimetry was performed with a MicroCal iTC200 Titration Calorimeter from Malvern (Palaiseau, France) and the data were analyzed using software Origin, Microcal Analysis Origin Launcher. The experiments were carried out at 15 °C. Aptamers and targets were dissolved in the same buffer, (see previous section for binding buffer composition, except for OTA, which was composed of 10 mM Tris, pH 8.5, 120 mM NaCl, 5 mM KCl, 20 mM $MgCl_2$, 3.66% ethanol). All the solutions were degassed to avoid air bubbles.

The aptamer concentration in the microcalorimeter cell (0.2 mL) varied from 8 to 30 μM. A total of 20 injections of 2 μL of target solution at concentrations varying from 300 to 500 μM were added at intervals of 120 s while stirring at 750 rpm. Control experiments were performed by injection of target into the buffer solution. At least two independent titrations were run.

3. Results

3.1. SYBR green displacement assays

The proof-of-principle of the SG-based FA strategy was previously established using the SG as probe and various functional DNA molecules as recognition elements. Three different model systems involving unstructured (23 mer) and hairpin-like (25 mer and 22 mer T-rich functional DNA) motifs were used for the respective detection of L-tyrosinamide, adenosine and Hg(II) (Fig. 1) [24]. As a function of the target nature and the induced-fit binding process of functional DNA, the mechanism is based on either the SG release or catch upon ligand binding. Therefore, positive or negative FA responses can be observed depending on the relative contributions of direct competition and allosteric switch processes.

This method was first applied using a 55 and a 35 mer aptamers named **SS2-55** and **SS-24**–**35** for the isocarbophos recognition (Fig. S1A). As expected, due to the short lifetime of the SYBR Green (in the picosecond range) relative to the time scale of rotation (in the subnanosecond range), the FA signal of the free dye was high, about 0.300 (data not shown). Upon complexation with the aptamer, the FA signal decreased with the dye/base ratio diminishing, as the result of both the considerable increase in τ (in the nanosecond range) and a resonance energy homotransfer (RET) effect between closely located dyes within DNA. The titration curves displayed a plateau within the 2–64 nM and 64–128 nM

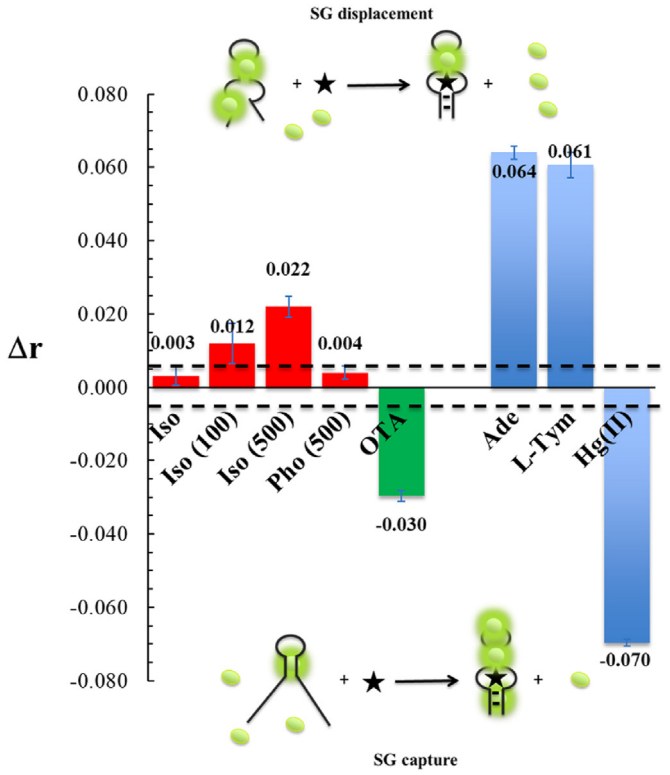

Fig. 1. Comparison of SG fluorescence anisotropy change Δr value for OP tested and other targets from this study or literature data:[40] In red colour: results obtained with aptamers dedicated to OP pesticide. In green colour: results with well-validated aptamers dedicated to small molecules. In blue colour: data from literature. The dotted line is the maximum standard deviation (s_D = 0.007) obtained from experiments conducted in the absence of targets (n = 20) **Iso** for 100 μM of isocarbophos with **SS2-55** aptamer, **Iso (100)**, **Iso (500)** and **Pho (500)** for respectively 100, 500 μM of isocarbophos and 500 μM of phorate with **SS24**–**35** aptamer. **Ade** for 1000 μM of Adenosine, **L-Tym** for 20 000 μM of L-tyrosinamide, **Hg(II)** for 312 nM of $HgCl_2$ and **OTA** for 25 μM of ochratoxin A. Experimental conditions for OP: Binding buffer: 10 mM Tris, pH 8, 50 mM NaCl, 10 mM KCl, 10 mM $MgCl_2$ and 5% ethanol, SG: 1.05 μM, Aptamers: 8 nM, reading immediately at room temperature for Iso and Iso (100), Reading after 30 min of incubation at 4 °C for Iso (500) and Pho (500). Experimental conditions for OTA: Binding buffer: 10 mM Tris, pH 8.5, 120 mM NaCl, 5 mM KCl, 20 mM $CaCl_2$ and 2.5% ethanol, SG: 1.05 μM, Aptamers: 2 μM, reading immediately at room temperature. (For interpretation of the references to colour in this figure legend, the reader is referred to the Web version of this article.)

ranges for **SS2-55** and **SS-24**–**35** aptamers, respectively, with a minimal value around 0.090–0.100. After this clear transition, an anisotropy increases higher for **SS2-55** than **SS-24**–**35** was observed with the DNA size increasing due to the enhancement in the apparent mass. Titration curves were established in the presence of 100 μM of isocarbophos (Fig. S1A) and then compared with those conducted in the absence of analyte. No difference in anisotropy was observed for **SS2-55** whereas we evidenced an Δr value of about 0.012 with the **SS-24**–**35** aptamer at 8 nM (Fig. 1). The distinct sequence length of the two oligonucleotides could explain the different behaviour between the two aptamers. Indeed, a higher length could induce the non-specific binding of SG to nucleobases that would be not implied in the target recognition process, leading to a detrimental effect on the FA response. This interpretation is supported by results reported in Fig. S1B, observed with Apt-Tym-38 (38 mer) and its truncated version Apt-Tym-23 (23 mer). A release of SG (Δr around 0.010) was recorded with Apt-Tym-38 whereas a greater extent of release occurred with Apt-Tym-23 (Δr around 0.020 for 100 μM of L-Tym) [24]. Nevertheless, the results obtained with Apt-Vaso-55 and Apt-Tym-49 indicated that SG displacement strategy is able to produce a FA change even if the sequence of aptamer was long (Fig. S1B). The minor Δr value of 0.003 at 100 μM isocarbophos, recorded using the **SS2-55** aptamer (Fig. 1:Iso) might suggest that the binding interaction of this aptamer was of lower magnitude than those of Apt-Vaso-55 and Apt-Tym-49 with (K_d of 1.1 μM [25] and 1.7 μM, respectively) [26].

As the temperature change is known to greatly impact the interaction of both the SG dye and the aptamer stability as well as the FA signal [24], 500 μM of isocarbophos or phorate was added to **SS-24**–**35** and reading measurements were performed after 30 min of incubation at 4 °C. For isocarbophos, the Δr value slightly increased with the target increasing concentration and temperature decreasing (from ~0.010 to ~0.020). Unfortunately, no difference in anisotropy was observed in the absence and presence of 500 μM of phorate, showing a negligible Δr value (Fig. 1). This indicates that phorate is unable to induce SYBR green displacement. The lack of response observed with phorate could originate from its different molecular structure as compared with isocarbophos. The aromatic residue, only retrieved in isocarbophos, could be able to interact with DNA through a larger interface and then displace more easily the SYBR green intercalator. It might be suspected that the target binds non-specifically to the functional DNA, explaining in turn the low Δr variation when the isocarbophos concentration was five-fold increased (from 100 to 500 μM). In contrast, a much enhanced Δr response was observed at saturation concentration with a variety of previously described aptamers involving hairpin, G-quadruplex or unstructured DNA motifs. The reported Δr values were respectively 0.064, 0.061, −0.070 or −0.030 for Ade, L-Tym, Hg(II) and OTA, respectively (Fig. 1). Of note, the saturation concentration obtained for Ade (1000 μM) was lower than that of LTym (20 000 μM). This difference had been explained by the occurrence of both SG release and capture mechanisms [24]. A similar mechanism for the **SS24**–**35** aptamer binding could occur.

3.2. Complementary strand displacement assays

Strand displacement assays based on a fluorescence anisotropy signal transduction approach was developed using the **SS-24**–**35** aptamer, as previously described for numerous compounds such as L-tyrosinamide [23], ATP [21], and ochratoxin [22]. This method exploits the ability of nucleic acids to generate duplex structures with complementary sequences (CS). In the absence of the target, base pairing between the complementary sequences of the aptamer and CS is privileged. Upon target addition, the aptamer reorganisation led to the aptamer-CS duplex destabilization, leading to the release of the CS that generates a detectable FA signal decrease.

Herein, two Texas red (TR)-labelled complementary strand (TR-CSA and TR-CSB) (Table 1) corresponding in large part to the sequence used in the original aptamer selection [10], were used as probes. On the basis of previous results obtained for L-tyrosinamide structure-switching assay [23], the Texas red fluorophore and a 9-mer CS were chosen to design the probe. It has been shown that, for a 12-mer CS, the fluorescein dye slightly raises the assay sensitivity as compared to the TR label, whereas the fluorescein labelled 9-mer CS does not afford the duplex formation with the aptamer. On the other hand, the same 9-mer CS tagged with the TR label is able to successfully form duplex with the functional oligonucleotide and is comfortably displaced upon target binding [23]. In addition to the length and the type of the fluorophore, another important parameter in the signal response is the CS:aptamer ratio [27]. For all the aptamers, the CS probe concentration was set to 20 nM and various aptamer concentrations ranging from 20 to 1280 nM were tested in the absence and presence of targets.

First, to verify that ethanol did not adversely affect the CS displacement, 5% of ethanol was added to the L-tyrosinamide

binding buffer. The titration curves (Fig. S2A) with the Apt-Tym concentration increasing were established using the TR-tagged CS previously described and 100 μM of L-tyrosinamide [23]. The addition of the target resulted in a large FA decrease for all the tested aptamer concentrations (with a Δr max value around −0.070 at 1280 nM of Apt-Tym-38). At the 320 nM aptamer concentration (1:16 CS:aptamer ratio), the CS displacement by the free target is optimal, indicating that a large amount of aptamer is favorable to the assay and showing that 5% ethanol affects neither the duplex formation nor the CS displacement. Of note, the aptamer concentration increase led to the Δr enhancement, better than that realised with the 1:1 CS:aptamer stoichiometry (Fig. 2: L-Tym *versus* L-Tym*).

For aptamer **SS24–35**, despite the presence of a higher salt concentration, weaker strength hybridization was observed with TR-CSA and TR-CSB as compared with the Apt-Tym–CS–Tym system (data not shown). In contrast to Apt-Tym, no displacement of either complementary strands TR-CSA or TR-CSB was observed for the **SS-24–35** aptamer in the presence of 500 μM of isocarbophos (Fig. S2A and Fig. 2) or 100 μM of phorate, and this, whatever the tested CS:aptamer ratio. Such finding is quite surprising because this strategy is known to be extremely generalisable and was successfully applied to various aptamers for L-Tym [23], ATP [21] or OTA [22], showing Δr value of −0.021, 0.023 or −0.017 respectively with 1:1 or 1:2 (for ATP) CS:aptamer ratio (Fig. 2). In addition, the molecular beacon employed in the original work of Zhang et al. [10] consisted of 20 bases where 15 of them are common to the two used CS.

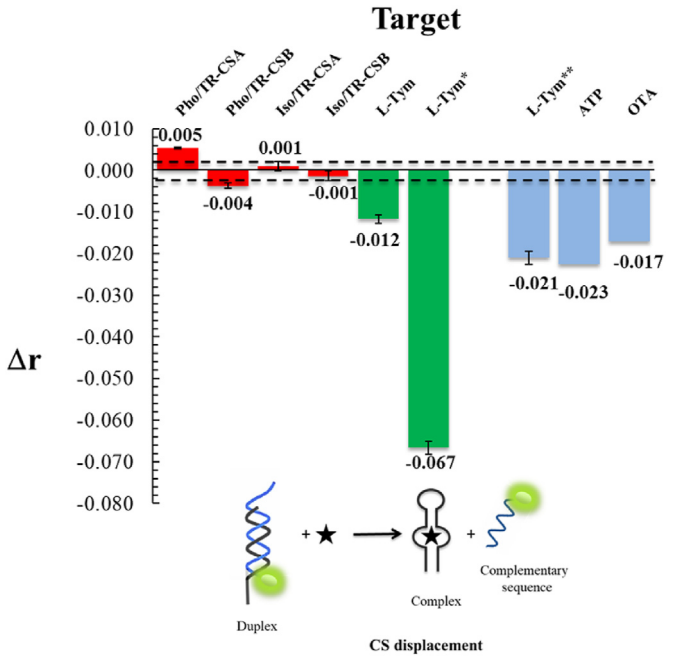

Fig. 2. Comparison of fluorescence anisotropy change Δr value for 500 μM of isocarbophos and 100 μM of phorate with CS displacement strategy with TR-CSA and TR-CSB on **SS24–35** aptamer and other small molecules from this study or literature data [21–23]. In red colour: results obtained with aptamers dedicated to OP pesticide. In green colour: results with well-validated aptamers dedicated to small molecules. In blue colour: data from literature. The dotted line is the maximum standard deviation ($s_D = 0.002$) obtained from experiments conducted in the absence of targets (n = 10). Experimental conditions for isocarbophos and phorate: CS concentration: 20 nM. SS24-35 aptamer: 320 nM; Binding buffer conditions: 10 mM Tris, pH 8, 50 mM NaCl, 10 mM KCl, 10 mM $MgCl_2$ and 5% ethanol. Experimental conditions for L-Tym: CS concentration: 20 nM. Apt-Tym aptamer: 20 nM or 320 nM (for L-Tym*) with 100 μM of L-tyrosinamide; 10 mM Tris, pH 7.5, 25 mM NaCl, 5 mM $MgCl_2$ and 5% ethanol.
Data literature conditions: [23]L-Tym**: CS concentration: 10 nM. Apt-Tym aptamer: 10 nM; L-Tym: 250 μM, 10 mM Tris, pH 7.5, 25 mM NaCl, 5 mM $MgCl_2$ [21]ATP: CS= PNA7-TR:200 nM, Aptamer: 400 nM; ATP: 500 μM, 10 mM Tris, pH 8.5, 10 mM NaCl, 10 mM $MgCl_2$ [22]Ochratoxin (OTA): CS: 10 nM, Aptamer: 10 nM, OTA: 110 nM, 10 mM TRIS pH 8.5, 120 mM NaCl, 20 mM $CaCl_2$, 5 mM KCl. (For interpretation of the references to colour in this figure legend, the reader is referred to the Web version of this article.)

The two FA displacement approaches developed herein failed to generate OP-dependent signals with the apparent affinities claimed by the authors. Theoretically, such lack of significant response can originate from two phenomena: (i) an ineffective reporting process and/or (ii) the inaptitude for the DNA molecules to bind the targets with the expected dissociation constants. Although of high generalizability features, the displacement signalling approaches may not work as well as intended in some cases. For example, Juncker et al. have demonstrated that a shorter CS, having a much lower hybridization free energy than the longer CS, displays no induced fit binding and may not be displaced by its target [28]. With this in mind, it might be possible that the 20 mer CS used by Zhang et al. [10] is moved more easily than our designed CS. Furthermore, the sensitivity of the SG displacement approach could be limited if the catch mechanism related to the DNA structuration upon target binding is significantly counterbalanced by a direct competitive effect [24].

3.3. ITC assays

In order to address the issues, we then decided to characterize the molecular recognition capabilities of the DNA molecules by using Isothermal titration calorimetry (ITC). ITC is a technique that directly measures the energetics associated with the binding of two components. Moreover, since heat is universally generated or absorbed during any molecular interaction, ITC has become a state-of-art label-free analytical method for characterizing small molecule aptamers [29]. When the affinity between the macromolecule and the ligand is comprised between 10^4 M^{-1} and 10^8 M^{-1} (100 μM < K_d < 0.01 μM), the affinity and the enthalpy of binding can be simultaneously determined in a single experiment. If the affinity between the reactants is too low (K_d > 100 μM), neither the affinity nor the enthalpy of binding can be reliably determined. Many examples of ITC-based binding affinity calculation for different small molecule-aptamer pairs have been successfully reported in the literature (Table 2).

Binding data for a variety of aptamers tested in literature are shown in Table 2 (in conditions similar to those realised with both OP and aptamers). In general, the aptamer concentration is comprised between 5 and 150 μM and the target concentration ranges from 25 to 900 μM, for dissociation constants comprised between 0.2 and 16 μM (as expected for isocarbophos and phorate). The aptamer Apt-Tym-38 was also tested with 5% of ethanol to verify that this percentage of organic solvent did not impact binding constant affinity determination by ITC.

The ITC profiles at 15 °C for the binding of the two pesticides (isocarbophos and phorate) to the two DNA aptamers are presented Fig. 3 and Fig. S3. Each of the heat burst curves corresponded to a single injection of the target solutions into the DNA solutions. The resulting heat plotted as a function of molar ratio was depicted in the lower panel where data points reflect the experimental injection heats while the solid lines reflect the calculated fits of the data. Unfortunately, the titration of **SS2-55 and SS24–35** aptamers by isocarbophos or phorate showed only minor heat exchange, in contrast with what is commonly reported in literature and recorded herein for L-Tym and OTA (Figs. S4 and S5). The titration of L-Tym to Apta-Tym-38 resulted in negative peaks that reveal exothermic binding. Data processing with the ITC software generated a K_d value of 0.5 ± 2.2 μM at 15 °C for L-tyrosinamide, in good agreement with the values of 0.63 ± 0.06 μM obtained for Apt-Tym-

Table 2
Examples of K_d determination and enthalpy change estimated by the ITC method for validated small molecule-aptamer systems. Non-exhaustive-list.

Small molecule	Aptamer bases structure	[small molecule] μM	[Aptamer] μM	Estimated K_d μM	ΔH kcal mol^{-1}	Ref
L-tyrosinamide	49	330	32	0.63 ± 0.06[a]	−16.1 ± 0.2	[30]
	23 unknown	250	15	0.19 ± 0.02[a]		
Adenosine	27 hairpin	500	10	16.4 ± 1.4	−14.1 ± 0.5	[54]
Cocaine	MN4	280	20	0.3 ± 0.1	−16 ± 3	[55]
	36					
	TWJ					
Cocaine	38-GC	500	20	2.6 ± 1.0	nd	[56]
	38					
	TWJ					
Quinine	MN4	230–2250	15 to 150	0.23 ± 0.03	−14.5 ± 0.4 nd	[57]
	TWJ	50	5	0.17 ± 0.04		[29]
Argininamide	Hairpin	7500	150	0.17 ± 0.015	nd	[29]
	24					
deoxycholic acid	WC	1200–4200	20 to 85	16 ± 3	−7 ± 1	[58]
	36					
	TWJ					
Iprobenfos	EIA2	25	0.5	1.67[b]	nd	[59]
Edifenphos	64			0.038[b]		
	Hairpin					
doxorubicin epirubicin daunorubicin	AS1411NT	900	5	1.24 ± 0.042	−7.9 ± 0.021	[60]
				2.22 ± 0.06	−7.9 ± 0.024	
				2.3 ± 0.06	−6.3 ± 0.019	

[a] At 15 °C; TWJ = Three Way junction; nd = not determined.
[b] s_D not determined.

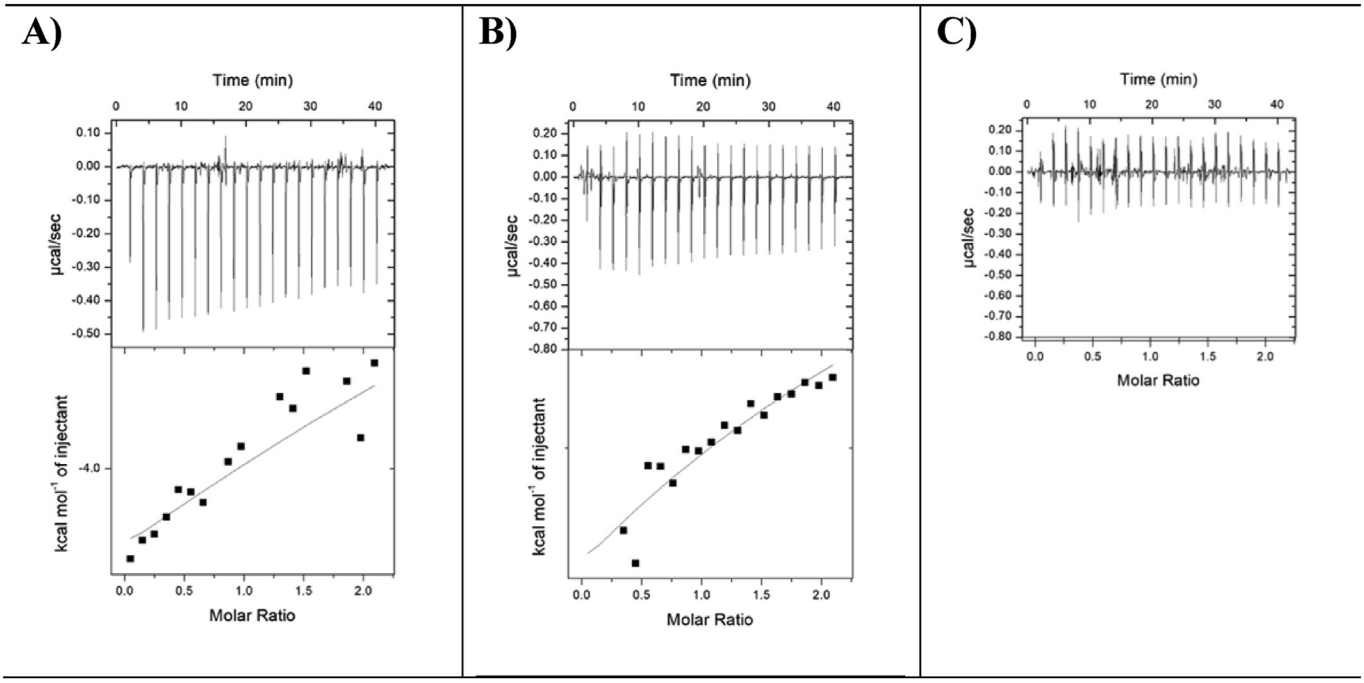

Fig. 3. ITC analysis of binding affinity of **SS2-55** (30 μM) **A)** and **SS24–35** (30 μM) **B)** with 300 μM isocarbophos **C)** Control: Titration of isocarbophos 300 μM in buffer solution. Experimental conditions: 50 mM Tris, pH 8, 50 mM NaCl, 10 mM KCl, 10 mM $MgCl_2$, 5% Ethanol. Temperature: 15 °C.

49 at the same temperature [30]. ITC results exhibit a lower enthalpy variation (−9.4 ± 0.3 kcal mol^{-1} *vs* −16.1 ± 0.2 kcal mol^{-1}) and a lower TΔS value (−0.35 kcal mol^{-1} *vs* −12.6 kcal mol^{-1}) as compared with Apt-Tym-49 [30]. Apart from the aptamer length difference, these distinct values could be attributed to the presence of 5% ethanol in the buffer. Control experiments performed by injection of L-tyrosinamide into the buffer solution yielded insignificant heats of dilution (Fig. S3).

From these data, we can conclude that, in homogeneous-phase, neither isocarbophos nor phorate display binding to **SS24–35** or **SS2-55** aptamers with dissociation constants in the micromolar range. These findings could explain the lack of significant displacement-based FA output upon binding of analytes under the current conditions.

4. Discussion and conclusion

Pesticide residue detection is a key approach for the management of pesticide contamination, which requires development of new methods for highly-sensitive detection. Under this

circumstance, novel aptamers have attracted great attention of researchers because of their well-known superiorities. Some publications have now highlighted the need to multiply characterization techniques of aptamers after the SELEX procedure as well as to carry out control experiments with scrambled sequences and non-cognate compounds to establish the aptamer binding and specificity.

In 2015, Mc Keague et al. have performed a comprehensive examination of a panel of traditional affinity binding assays using a set of aptamers for the small molecule target, ochratoxin A. They proposed a workflow that allows specific recommendations for each step of the *in vitro* procedure (*i.e.* aptamer screening, characterization, and functional validation for optimal integration into Aptamer-Based Applications) that will ensure that new aptamers are entirely and securely characterized [31]. The characterization is a key step of the whole SELEX procedure and the multiplication of different binding evaluation procedures between an aptamer and its target is an essential prerequisite for further aptamer use.

Some model aptamers devoted to small molecules such as adenosine [32], L-tyrosinamide [33], cocaine [34], or ochratoxin A [35] have proved their worth in the development of the different biosensor platforms. As an example, the anti-adenosine aptamer was studied in all directions with different transduction approaches as electrochemical, mass-based [36] and optical like fluorescence anisotropy (FA). For instance, in FA approach, different strategies involving direct [37], split assembly [38], kissing assembly [39], enzymatic protection [40] nanomaterial amplification [41], protein amplification [42], recycling amplification [43], or dye displacement [44] were successfully applied, highlighting the performant selection and the binding recognition properties of such functional DNA molecules.

From the aptamer selection to the biosensor design, there are many check points that guarantee the analytical results, such as the employment of scrambled DNA sequences, the choice of concurrent analytes as controls and independent methods for binding constant determination. Recently, Zong and Liu have performed large binding assays on the arsenic binding aptamer named Ars-3 using ITC, DNA staining dyes, and gold nanoparticles (AuNPs). After carefully comparing Ars-3 and a few random control DNA sequences, they concluded that Ars-3 does not recognize As(III) [45]. Some authors have highlighted that gold nanoparticles can bind to different targets [46]. For example, the adsorption of As(III) on the AuNP surface [47] can produce the exact same colour response for colorimetric sensing than the positive assay (+ target) with aptamer, creating artefacts in AuNP-based biosensors. This publication challenges about the characterization of certain aptamers for which there is a lack of controls. More recently, De Wael et al. have compared different analytical methodologies to validate or disprove the binding capabilities of ampicillin-binding aptamer sequences. The target binding potential was evaluated in solution using ITC, native nano-electrospray ionization mass spectrometry and 1H nuclear magnetic resonance spectroscopy. Here again, the authors concluded that there are no reasons to believe that complexation occurs within the low nM to high mM range [29].

Regarding the anti-pesticide aptamers investigated in the present work, rare are the studies for which all the controls were carried out. Only one publication related to the OP determination exhibits adequate controls to reveal the binding interaction between the **SS24**–**35** and omethoate [16]. For other ones, including the one by Wang et al. [9], control experiments are missing. In most cases, pesticides analogues are used to test the aptasensor specificity; however, no investigation with scrambled sequences and target alone in the presence of sensing materials is conducted [11,14–16] At best, analogous pesticides and/or scrambled sequences [17] are examined but the effects of the target adsorption onto the AuNP surface are rarely investigated [13].

The response of an aptamer in solution can be significantly different from that reported with the same functional oligonucleotide immobilized onto a biosensor surface. For examples, several studies on microarrays have reported differences in aptamer affinity when compared with solution-based measurements [48]. Positively charged surfaces, immobilisation densities, aptamer orientations as well as spacer moieties may directly influence aptamer's folding and consequently binding [49]. Manipulation of the conditions (specific incubation times, temperatures and buffer conditions as well as the presence of blocking agents to decrease non-specific binding) can promote the interaction of weak binding sequences with their target, where binding was not previously observed [50]. In addition, surface-based interaction can be improved relative to solution-based binding through enhancement in the local concentration. As shown for IgE in SPRi, the amount of target bound goes through a maximum as function of the aptamer surface density. In the low surface density range, the target binding increases with the aptamer surface density until the limit of steric hindrance is reached in the bound target layer. After that, the bound IgE amount decreases as the aptamer surface density is further increased [51].

Thus, the results obtained in this study highlighted the necessity to validate the binding potential of new isolated aptamers various and complementary techniques involving homogeneous methods, which avoid surface effects. This is especially important for aptamers that bind to small molecules. Recently, for a published aptamer dedicated to a protein target, the authors went in the right direction by portraying affinity measurements performed with three different techniques combining heterogeneous (SPR) and homogeneous (Microscale Thermophoresis and filter radiolabelling) platform in three independent laboratories as it was advised by Famulok and Mayer [52,53].

CRediT authorship contribution statement

Lorena Zara: Investigation, Methodology, Validation, Visualization. **Silvia Achilli:** Investigation. **Benoît Chovelon:** Investigation. **Emmanuelle Fiore:** Investigation, Resources. **Jean-Jacques Toulmé:** Reviewing, Supervision. **Eric Peyrin:** Conceptualization, Writing – review & editing, Supervision. **Corinne Ravelet:** Conceptualization, Writing, Supervision.

Declaration of competing interest

The authors declare that they have no known competing financial interests or personal relationships that could have appeared to influence the work reported in this paper.

Acknowledgments

We thank Emilie Gillon and Anne Imberty for respectively providing helpful technical support and discussion about ITC experiments and data analysis.

This work was supported by funding ANRT CIFRE.

This work has been partially supported by the PolyNatCarnot Institute (Investissements d'Avenir -grant agreement n°ANR-11-CARN-007-01).

Appendix A. Supplementary data

Supplementary data to this article can be found online at https://doi.org/10.1016/j.aca.2021.338382.

References

[1] R. Mahajan, M.R. Bonner, J.A. Hoppin, M.C.R. Alavanja, Phorate exposure and incidence of cancer in the agricultural health study, Environ. Health Perspect. 114 (2006) 1205–1209.

[2] M. Jia, Y. Wang, M. Teng, D. Wang, J. Yan, J. Miao, Z. Zhou, W. Zhu, Toxicity and metabolomics study of isocarbophos in adult zebrafish (Danio rerio), Ecotoxicol. Environ. Saf. 163 (2018) 1–6.

[3] S. Rodriguez-Mozaz, M.J.L. de Alda, D. Barceló, Monitoring of estrogens, pesticides and bisphenol A in natural waters and drinking water treatment plants by solid-phase extraction-liquid chromatography-mass spectrometry, J. Chromatogr. A 1045 (2004) 85–92.

[4] I. Ferrer, E.M. Thurman, Multi-residue method for the analysis of 101 pesticides and their degradates in food and water samples by liquid chromatography/time-of-flight mass spectrometry, J. Chromatogr. A 1175 (2007) 24–37.

[5] L. Wu, Y. Song, M. Hu, H. Zhang, A. Yu, C. Yu, Q. Ma, Z. Wang, Application of magnetic solvent bar liquid-phase microextraction for determination of organophosphorus pesticides in fruit juice samples by gas chromatography mass spectrometry, Food Chem. 176 (2015) 197–204.

[6] S. Rodriguez-Mozaz, M.J. Lopez de Alda, D. Barceló, Advantages and limitations of on-line solid phase extraction coupled to liquid chromatography-mass spectrometry technologies versus biosensors for monitoring of emerging contaminants in water, J. Chromatogr. A 1152 (2007) 97–115.

[7] V.-T. Nguyen, Y.S. Kwon, M.B. Gu, Aptamer-based environmental biosensors for small molecule contaminants, Curr. Opin. Biotechnol. 45 (2017) 15–23.

[8] M. Liu, A. Khan, Z. Wang, Y. Liu, G. Yang, Y. Deng, N. He, Aptasensors for pesticide detection, Biosens. Bioelectron. 130 (2019) 174–184, https://doi.org/10.1016/j.bios.2019.01.006.

[9] L. Wang, X. Liu, Q. Zhang, C. Zhang, Y. Liu, K. Tu, J. Tu, Selection of DNA aptamers that bind to four organophosphorus pesticides, Biotechnol. Lett. 34 (2012) 869–874.

[10] C. Zhang, L. Wang, Z. Tu, X. Sun, Q. He, Z. Lei, C. Xu, Y. Liu, X. Zhang, J. Yang, X. Liu, Y. Xu, Organophosphorus pesticides detection using broad-specific single-stranded DNA based fluorescence polarization aptamer assay, Biosens. Bioelectron. 55 (2014) 216–219.

[11] S. Pang, T.P. Labuza, L. He, Development of a single aptamer-based surface enhanced Raman scattering method for rapid detection of multiple pesticides, The Analyst 139 (2014) 1895–1901.

[12] J. Fu, X. An, Y. Yao, Y. Guo, X. Sun, Electrochemical aptasensor based on one step co-electrodeposition of aptamer and GO-CuNPs nanocomposite for organophosphorus pesticide detection, Sensor. Actuator. B Chem. 287 (2019) 503–509.

[13] W. Bai, C. Zhu, J. Liu, M. Yan, S. Yang, A. Chen, Gold nanoparticle-based colorimetric aptasensor for rapid detection of six organophosphorous pesticides, Environ. Toxicol. Chem. 34 (2015) 2244–2249.

[14] R. Bala, R.K. Sharma, N. Wangoo, Development of gold nanoparticles-based aptasensor for the colorimetric detection of organophosphorus pesticide phorate, Anal. Bioanal. Chem. 408 (2016) 333–338.

[15] D.-L. Liu, Y. Li, R. Sun, J.-Y. Xu, Y. Chen, C.-Y. Sun, Colorimetric detection of organophosphorus pesticides based on the broad-spectrum aptamer, J. Nanosci. Nanotechnol. 20 (2020) 2114–2121.

[16] P. Wang, Y. Wan, A. Ali, S. Deng, Y. Su, C. Fan, S. Yang, Aptamer-wrapped gold nanoparticles for the colorimetric detection of omethoate, Sci. China Chem. 59 (2016) 237–242.

[17] X. Li, J. Shi, C. Chen, W. Li, L. Han, L. Lan, Y. Guo, Y. Chang, J. Cai, Y. Ding, One-step, visual and sensitive detection of phorate in blood based on a DNA–AgNC aptasensor, New J. Chem. 42 (2018) 6293–6298.

[18] R. Nutiu, Y. Li, Aptamers with fluorescence-signaling properties, Methods San Diego Calif 37 (2005) 16–25.

[19] B. Juskowiak, Nucleic acid-based fluorescent probes and their analytical potential, Anal. Bioanal. Chem. 399 (2011) 3157–3176.

[20] T. Li, E. Wang, S. Dong, G-Quadruplex-based DNAzyme as a sensing platform for ultrasensitive colorimetric potassium detection, Chem. Commun. (2009) 580–582.

[21] E. Goux, Q. Lespinasse, V. Guieu, S. Perrier, C. Ravelet, E. Fiore, E. Peyrin, Fluorescence anisotropy-based structure-switching aptamer assay using a peptide nucleic acid (PNA) probe, Methods 97 (2016) 69–74, https://doi.org/10.1016/j.ymeth.2015.09.018.

[22] J.A. Cruz-Aguado, G. Penner, Fluorescence polarization based displacement assay for the determination of small molecules with aptamers, Anal. Chem. 80 (2008) 8853–8855.

[23] Z. Zhu, T. Schmidt, M. Mahrous, V. Guieu, S. Perrier, C. Ravelet, E. Peyrin, Optimization of the structure-switching aptamer-based fluorescence polarization assay for the sensitive tyrosinamide sensing, Anal. Chim. Acta 707 (2011) 191–196.

[24] B. Chovelon, E. Fiore, P. Faure, E. Peyrin, C. Ravelet, A lifetime-sensitive fluorescence anisotropy probe for DNA-based bioassays: the case of SYBR Green, Biosens. Bioelectron. 90 (2017) 140–145.

[25] K.P. Williams, X.-H. Liu, T.N.M. Schumacher, H.Y. Lin, D.A. Ausiello, P.S. Kim, D.P. Bartel, Bioactive and nuclease-resistant l-DNA ligand of vasopressin, Proc. Natl. Acad. Sci. U. S. A. 94 (1997) 11285–11290.

[26] J. Ruta, S. Perrier, C. Ravelet, J. Fize, E. Peyrin, Noncompetitive fluorescence polarization aptamer-based assay for small molecule detection, Anal. Chem. 81 (2009) 7468–7473.

[27] Y. Li, Q. Zhao, Aptamer structure switch fluorescence anisotropy assay for small molecules using streptavidin as an effective signal amplifier based on proximity effect, Anal. Chem. 91 (2019) 7379–7384.

[28] J.D. Munzar, A. Ng, M. Corrado, D. Juncker, Complementary oligonucleotides regulate induced fit ligand binding in duplexed aptamers, Chem. Sci. 8 (2017) 2251–2256.

[29] F. Bottari, E. Daems, A.-M. de Vries, P. Van Wielendaele, S. Trashin, R. Blust, F. Sobott, A. Madder, J.C. Martins, K. De Wael, Do aptamers always bind? The need for a multifaceted analytical approach when demonstrating binding affinity between aptamer and low molecular weight compounds, J. Am. Chem. Soc. 142 (2020) 19622–19630.

[30] L. Challier, R. Miranda-Castro, B. Barbe, C. Fave, B. Limoges, E. Peyrin, C. Ravelet, E. Fiore, P. Labbe, L. Coche-Guerente, E. Ennifar, G. Bec, P. Dumas, F. Mavre, V. Noel, Multianalytical study of the binding between a small chiral molecule and a DNA aptamer: evidence for asymmetric steric effect upon 3 '-versus 5 '-End sequence modification, Anal. Chem. 88 (2016) 11963–11971.

[31] M. McKeague, A. De Girolamo, S. Valenzano, M. Pascale, A. Ruscito, R. Velu, N.R. Frost, K. Hill, M. Smith, E.M. McConnell, M.C. DeRosa, Comprehensive analytical comparison of strategies used for small molecule aptamer evaluation, Anal. Chem. 87 (2015) 8608–8612.

[32] D.E. Huizenga, J.W. Szostak, A DNA aptamer that binds adenosine and ATP, Biochemistry 34 (1995) 656–665.

[33] E. Vianini, M. Palumbo, B. Gatto, In vitro selection of DNA aptamers that bind L-tyrosinamide, Bioorg, Med. Chem. 9 (2001) 2543–2548.

[34] M.N. Stojanovic, P. de Prada, D.W. Landry, Fluorescent sensors based on aptamer self-assembly, J. Am. Chem. Soc. 122 (2000) 11547–11548, https://doi.org/10.1021/ja0022223.

[35] J.A. Cruz-Aguado, G. Penner, Determination of ochratoxin A with a DNA aptamer, J. Agric. Food Chem. 56 (2008) 10456–10461.

[36] J. Wang, A. Munir, H.S. Zhou, Au NPs-aptamer conjugates as a powerful competitive reagent for ultrasensitive detection of small molecules by surface plasmon resonance spectroscopy, Talanta 79 (2009) 72–76.

[37] S. Perrier, C. Ravelet, V. Guieu, J. Fize, B. Roy, C. Perigaud, E. Peyrin, Rationally designed aptamer-based fluorescence polarization sensor dedicated to the small target analysis, Biosens. Bioelectron. 25 (2010) 1652–1657.

[38] Z. Zhu, C. Ravelet, S. Perrier, V. Guieu, E. Fiore, E. Peyrin, Single-Stranded DNA binding protein-assisted fluorescence polarization aptamer assay for detection of small molecules, Anal. Chem. 84 (2012) 7203–7211.

[39] G. Durand, S. Lisi, C. Ravelet, E. Dausse, E. Peyrin, J.-J. Toulme, Riboswitches based on kissing complexes for the detection of small ligands, Angew. Chem. Int. Ed. 53 (2014) 6942–6945.

[40] A. Kidd, V. Guieu, S. Perrier, C. Ravelet, E. Peyrin, Fluorescence polarization biosensor based on an aptamer enzymatic cleavage protection strategy, Anal. Bioanal. Chem. 401 (2011) 3229–3234.

[41] X. Xiao, Y.F. Li, C.Z. Huang, S.J. Zhen, A novel graphene oxide amplified fluorescence anisotropy assay with improved accuracy and sensitivity, Chem. Commun. 51 (2015) 16080–16083.

[42] L. Kang, B. Yang, X. Zhang, L. Cui, H. Meng, L. Mei, C. Wu, S. Ren, W. Tan, Enzymatic cleavage and mass amplification strategy for small molecule detection using aptamer-based fluorescence polarization biosensor, Anal. Chim. Acta 879 (2015) 91–96.

[43] Y. Huang, X. Liu, L. Zhang, K. Hu, S. Zhao, B. Fang, Z.-F. Chen, H. Liang, Nicking enzyme and graphene oxide-based dual signal amplification for ultrasensitive aptamer-based fluorescence polarization assays, Biosens. Bioelectron. 63 (2015) 178–184.

[44] B. Chovelon, E. Fiore, P. Faure, E. Peyrin, C. Ravelet, A lifetime-sensitive fluorescence anisotropy probe for DNA-based bioassays: the case of SYBR Green, Biosens. Bioelectron. 90 (2017) 140–145.

[45] C. Zong, J. Liu, The arsenic-binding aptamer cannot bind arsenic: critical evaluation of aptamer selection and binding, Anal. Chem. 91 (2019) 10887–10893.

[46] Q. Shao, C.K. Hall, Binding preferences of amino acids for gold nanoparticles: a molecular simulation study, Langmuir ACS J. Surf. Colloids. 32 (2016) 7888–7896.

[47] C. Zong, Z. Zhang, B. Liu, J. Liu, Adsorption of arsenite on gold nanoparticles studied with DNA oligonucleotide probes, Langmuir ACS J. Surf. Colloids. 35 (2019) 7304–7311.

[48] J.A. Martin, Y. Chushak, J.L. Chávez, J.A. Hagen, N. Kelley-Loughnane, Microarrays as model biosensor platforms to investigate the structure and affinity of aptamers, J. Nucleic Acids (2016) 1–11.

[49] K. Urmann, J. Modrejewski, T. Scheper, J.-G. Walter, Aptamer-modified nanomaterials: principles and applications, BioNanoMaterials 18 (2017) 1–17.

[50] E. Katilius, C. Flores, N.W. Woodbury, Exploring the sequence space of a DNA aptamer using microarrays, Nucleic Acids Res. 35 (2007) 7626–7635.

[51] L. Simon, Z. Bognár, R.E. Gyurcsányi, Finding the optimal surface density of aptamer monolayers by SPR imaging detection-based aptamer microarrays, Electroanalysis 32 (2020) 851–858.

[52] M. Jauset Rubio, M. Svobodová, T. Mairal, T. Schubert, S. Künne, G. Mayer, C.K. O'Sullivan, β-Conglutin dual aptamers binding distinct aptatopes, Anal. Bioanal. Chem. 408 (2016) 875–884.

[53] M. Famulok, G. Mayer, Aptamers and SELEX in chemistry & biology, Chem. Biol. 21 (2014) 1055–1058.

[54] Z. Zhang, O. Oni, J. Liu, New insights into a classic aptamer: binding sites,

cooperativity and more sensitive adenosine detection, Nucleic Acids Res. 45 (2017) 7593–7601.
[55] M.A.D. Neves, O. Reinstein, M. Saad, P.E. Johnson, Defining the secondary structural requirements of a cocaine-binding aptamer by a thermodynamic and mutation study, Biophys. Chem. 153 (2010) 9–16.
[56] D. Roncancio, H. Yu, X. Xu, S. Wu, R. Liu, J. Debord, X. Lou, Y. Xiao, A label-free aptamer-fluorophore assembly for rapid and specific detection of cocaine in biofluids, Anal. Chem. 86 (2014) 11100–11106.
[57] O. Reinstein, M. Yoo, C. Han, T. Palmo, S.A. Beckham, M.C.J. Wilce, P.E. Johnson, Quinine binding by the cocaine-binding aptamer. Thermodynamic and hydrodynamic analysis of high-affinity binding of an off-target ligand, Biochemistry 52 (2013) 8652–8662.
[58] O. Reinstein, M.A.D. Neves, M. Saad, S.N. Boodram, S. Lombardo, S.A. Beckham, J. Brouwer, G.F. Audette, P. Groves, M.C.J. Wilce, P.E. Johnson, Engineering a structure switching mechanism into a steroid-binding aptamer and hydrodynamic analysis of the ligand binding mechanism, Biochemistry 50 (2011) 9368–9376.
[59] Y.S. Kwon, V.-T. Nguyen, J.G. Park, M.B. Gu, Detection of iprobenfos and edifenphos using a new multi-aptasensor, Anal. Chim. Acta 868 (2015) 60–66.
[60] W. Pei, M. Liu, Y. Wu, Y. Zhao, T. Liu, B. Sun, Y. Liu, Q. Wang, J. Han, High payload and targeted release of anthracyclines by aptamer-tethered DNA nanotrains — thermodynamic and release kinetic study, Eur. J. Pharmaceut. Sci. 148 (2020) 105319.